Preprints of the 18th IFAC World Congress
Milano (Italy) August 28 - September 2, 2011

Optimal Squeezing using Multivariable Integral LQG Control ⋆

S. Z. Sayed Hassen, * **I. R. Petersen, E. H. Huntington** **

* *University of Mauritius, Réduit, Mauritius (sayed.hassen@gmail.com)*
** *University of New South Wales at ADFA, Canberra, Australia (i.r.petersen@gmail.com, e.huntington@adfa.edu.au)*

Abstract: In quantum optics, squeezed states of light can be generated in a nonlinear process by using an optical parametric oscillator (OPO). It is necessary however that the resonator cavity of the OPO maintain a frequency-lock, while at the same time sufficiently suppress classical noises in a chosen optical quadrature. In this paper, we model such an optical system and design an LQG optimal multivariable controller (which includes integral action) that satisfies the practical constraints imposed by this problem.

1. INTRODUCTION

It is well known in the physics literature that experiments performed at the quantum level are restricted by quantum noises. The quantum noise limit (QNL) sets a fundamental limit on the performance of quantum systems and puts a bound on the signal to noise ratio that can be achieved, thus restricting the usefulness of applications involving quantum technology. In quantum optics, the noise distribution of a quantum state of light can however be rearranged if we concentrate the quantum noises in specific quadratures of light (see Bachor and Ralph [2004]). In such cases, one quadrature has less noise than the other and quantum states of light which possess this property of asymmetric quadrature noise distributions are known as "squeezed" or "non-classical" states of light.

The statistics of quantum noises can be altered through the use of nonlinear effects (see Boyd [2008]) in quantum optics, allowing for measurements that are better than permitted by the standard quantum limit (SQL). Here, the SQL refers to the minimum level of quantum noise that can be obtained with the use of coherent states of light that possess "classical" quantum noise properties. This uncertainty, which can be visualised as corresponding to a circular and symmetric area, restricts how close two measurable quantum states can be if they are to be distinguished from each other. Indeed, classical noises affect measurement of classical states in a similar fashion. However, classical noises can (in theory) be completely suppressed with improved measurement techniques. This is not the case for quantum noises whose sizes are dictated by the laws of quantum mechanics rather than as a result of the limitations of the measurement devices.

One application of squeezed states of light is in gravitational wave detection (see Caves [1981]) where the use of phase-squeezed light allows for a reduction in the necessary laser power to achieve a given signal to noise ratio. Other applications include quantum teleportation, quantum communication and quantum key distribution.

In this paper, we extend the work performed in Sayed Hassen et al. [2010] to the multivariable case. In addition to the original requirement of optimising the level of observed squeezing in a chosen quadrature, we also include the requirement of minimizing the detuning variables (see Bachor and Ralph [2004] and Sayed Hassen et al. [2009]). Having a multivariable controller which combines both performance objectives, allows interactions between possibly conflicting requirements to be systematically accounted for. This can potentially result in considerable performance improvement in the level of squeezing observed.

2. MODELLING

An optical parametric oscillator (OPO) consists of a second-order nonlinear optical medium enclosed within an optical resonator. Materials showing second-order nonlinearities $\chi^{(2)}$ have the ability to couple a fundamental field (f) to a second harmonic field ($2f$). Feedback in a resonator cavity results in the coherent build-up of the field inside the resonator thereby increasing the strength of the nonlinearity to levels useful for continuous-wave experiments. The OPO ensures phase-sensitive amplification of the quadratures of light such that noise in one quadrature is amplified and de-amplified in the orthogonal quadrature; see Bachor and Ralph [2004]; Gardiner and Zoller [2000]; Boyd [2008].

2.1 Optical Resonator Cavity

A schematic of an OPO driven by two optical fields $\hat{A}_{in}$ and $\hat{B}_{in}$ is shown in Fig. 1.

The quantities $\hat{A}_{in}$ and $\hat{B}_{in}$ are the input fields which setup the fundamental and second-harmonic intracavity fields $\hat{a}$ and $\hat{b}$. $\kappa_{a,in}$ and $\kappa_{b,in}$ represent the loss rates of the input/output mirrors for the $\hat{a}$ and $\hat{b}$ fields respectively.

⋆ This work is supported by the Australian Research Council and the Research Publication Fellowship.

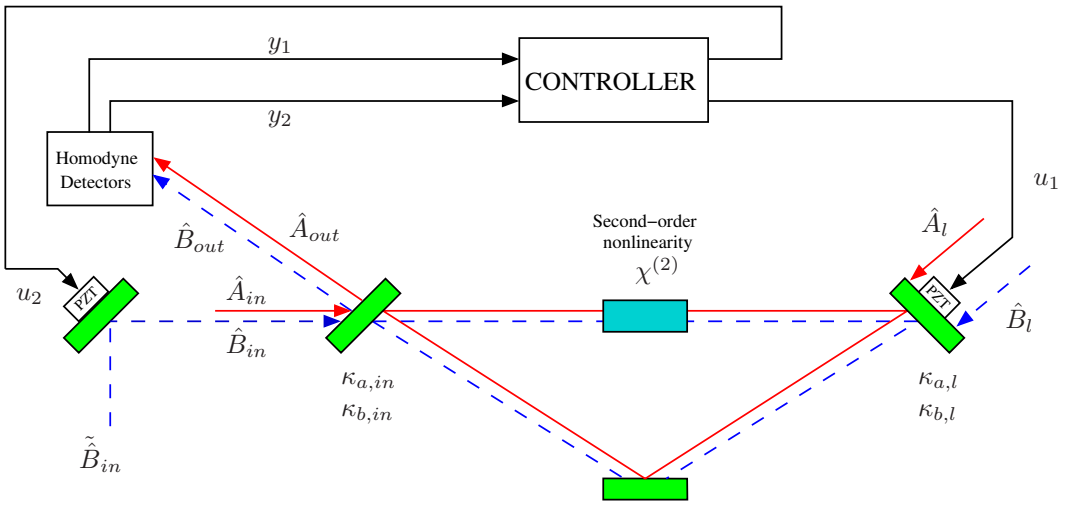

Fig. 1. Schematic of the proposed multivariable controller for the Optical Parametric Oscillator.

The parameters $\kappa_{a,l}$ and $\kappa_{b,l}$ are the internal loss rates for the corresponding two fields. Also, $\kappa_a = \kappa_{a,in} + \kappa_{a,l}$ and $\kappa_b = \kappa_{b,in} + \kappa_{b,l}$ are the associated total resonator decay rates. Furthermore, $\delta\hat{A}_l$ and $\delta\hat{B}_l$ represent the vacuum fields due to the internal losses. The output fields are given by $\hat{A}_{out}$ and $\hat{B}_{out}$.

The quantum mechanical Hamiltonian describing the second-order nonlinear ($\chi^{(2)}$) interactions is given by

$$\hat{H} = i\chi^{(2)}(\hat{b}^\dagger\hat{a}^2 - \hat{a}^{\dagger 2}\hat{b}), \tag{1}$$

where $a(a^\dagger)$ and $b(b^\dagger)$ are the annihilation (creation) operators for the fundamental and second harmonic fields respectively; see Bachor and Ralph [2004].

Using a canonical quantisation of the equations of motion of a ring cavity (a procedure first undertaken by P. Dirac) and combining it with the Heisenberg equations of motion, we obtain the dynamics of the OPO for the internal cavity modes as (see Collett and Gardiner [1984]):

$$\dot{\hat{a}} = -(\kappa_a + i\Delta_a)\hat{a} + \chi^{(2)}\hat{a}^\dagger\hat{b} + \sqrt{2\kappa_{a,in}}\hat{A}_{in} + \sqrt{2\kappa_{a,l}}\delta\hat{A}_l;$$
$$\dot{\hat{b}} = -(\kappa_b + i\Delta_b)\hat{b} - \frac{1}{2}\chi^{(2)}\hat{a}^2 + \sqrt{2\kappa_{b,in}}\hat{B}_{in} + \sqrt{2\kappa_{b,l}}\delta\hat{B}_l;$$

where Δ_a and Δ_b represent frequency mismatches (detuning variables). Detuning variables are defined as the difference between the respective resonant frequency of the cavity and the frequency of the incoming laser beams. The output fields are given by:

$$\hat{A}_{out} = \sqrt{2\kappa_{a,in}}\hat{a} - \hat{A}_{in}; \tag{2}$$
$$\hat{B}_{out} = \sqrt{2\kappa_{b,in}}\hat{b} - \hat{B}_{in}. \tag{3}$$

2.2 System Description using Quadrature Operators

The amplitude and phase quadrature operators provide for a useful description of the properties of light. We define them here for the optical fields $\hat{a}$ and $\hat{b}$:

$$X_a^+ = \hat{a} + \hat{a}^\dagger; \quad X_a^- = i(\hat{a}^\dagger - \hat{a}); \tag{4}$$
$$X_b^+ = \hat{b} + \hat{b}^\dagger; \quad X_b^- = i(\hat{b}^\dagger - \hat{b}). \tag{5}$$

The quadratures of the input and noise fields can similarly be defined and we can rewrite the nonlinear dynamics of the optical subsystem in terms of the quadratures. While the nonlinear properties are essential for the generation of squeezed states of light, we only need to consider first order terms in the variations to obtain elliptical contours and Gaussian distribution functions for the states. In this way, we can linearise the dynamics of the optical subsystem without losing the important characteristic features of the optical squeezer and model the behaviour of the system for small perturbations about a steady state operating point of the system. The linearised dynamics of the OPO are thus determined as:

$$\begin{aligned}\delta\dot{X}_a^+ = &-\kappa_a\delta X_a^+ + \bar{X}_a^-\Delta_a + \frac{1}{2}\chi^{(2)}(\bar{X}_b^+\delta X_a^+ + \bar{X}_b^-\delta X_a^-)\\ &+ \frac{1}{2}\chi^{(2)}(\bar{X}_a^+\delta X_b^+ + \bar{X}_a^-\delta X_b^-)\\ &+\sqrt{2\kappa_{a,in}}\delta X_{Ain}^+ + \sqrt{2\kappa_{a,l}}X_{\delta A,l}^+;\end{aligned} \tag{6}$$

$$\begin{aligned}\delta\dot{X}_a^- = &-\kappa_a\delta X_a^- - \bar{X}_a^+\Delta_a + \frac{1}{2}\chi^{(2)}(\bar{X}_b^-\delta X_a^+ - \bar{X}_b^+\delta X_a^-)\\ &+ \frac{1}{2}\chi^{(2)}(-\bar{X}_a^-\delta X_b^+ + \bar{X}_a^+\delta X_b^-)\\ &+\sqrt{2\kappa_{a,in}}\delta X_{Ain}^- + \sqrt{2\kappa_{a,l}}X_{\delta A,l}^-;\end{aligned} \tag{7}$$

$$\begin{aligned}\delta\dot{X}_b^+ = &-\kappa_b\delta X_b^+ + \bar{X}_b^-\Delta_b - \frac{1}{2}\chi^{(2)}(\bar{X}_a^+\delta X_a^+ - \bar{X}_a^-\delta X_a^-)\\ &+\sqrt{2\kappa_{b,in}}\delta X_{Bin}^+ + \sqrt{2\kappa_{b,l}}X_{\delta B,l}^+;\end{aligned} \tag{8}$$

$$\begin{aligned}\delta\dot{X}_b^- = &-\kappa_b\delta X_b^- - \bar{X}_b^+\Delta_b - \frac{1}{2}\chi^{(2)}(\bar{X}_a^-\delta X_a^+ + \bar{X}_a^+\delta X_a^-)\\ &+\sqrt{2\kappa_{b,in}}\delta X_{Bin}^- + \sqrt{2\kappa_{b,l}}X_{\delta B,l}^-.\end{aligned} \tag{9}$$

Also, the corresponding linearised output field equations are expressed as

$$\delta X_{Aout}^\pm = \sqrt{2\kappa_{a,in}}\delta X_a^\pm - \delta X_{Ain}^\pm; \tag{10}$$
$$\delta X_{Bout}^\pm = \sqrt{2\kappa_{b,in}}\delta X_b^\pm - \delta X_{Bin}^\pm. \tag{11}$$

Here, $\bar{X}_a^+, \bar{X}_a^-, \bar{X}_b^+$ and $\bar{X}_b^-$ denote the steady-state values of the respective quadratures. These are determined for the given set of input fields and phase angles by solving

the nonlinear coupled equations obtained by setting the derivatives in the nonlinear equations to zero.

3. STEADY-STATE CONDITIONS NECESSARY FOR SQUEEZING

At steady-state, there is a constant flow of energy between the intracavity optical fields. For the optical squeezer under consideration, the flow of energy is predominantly from the second-harmonic field to the fundamental field. In Sayed Hassen et al. [2010], we determined the relationship that exists between the phase of the intracavity fields and the type of squeezed states obtained. We showed in Sayed Hassen et al. [2010] that to achieve optimal amplitude quadrature squeezing, we would choose the operating point so that

$$\bar{\theta}_{b,in} - 2\bar{\theta}_{a,in} = n\pi; \quad \text{where } n \in \mathbb{Z}. \tag{12}$$

Here, $\bar{\theta}_{a,in}$ and $\bar{\theta}_{b,in}$ denote the steady-state phase angles of the input fields $\hat{A}_{in}$ and $\hat{B}_{in}$ respectively. Furthermore, the relationships between $\bar{\theta}_{a,in}$ and $\bar{\theta}_a$ and between $\bar{\theta}_{b,in}$ and $\bar{\theta}_b$ show that an equivalent condition to (12) for maximum amplitude squeezing of the fundamental intracavity field $\hat{a}$ is

$$\bar{\theta}_b - 2\bar{\theta}_a = n\pi. \tag{13}$$

Here, $\bar{\theta}_a$ and $\bar{\theta}_b$ denote the steady-state phase angles of the intracavity fields $\hat{a}$ and $\hat{b}$ respectively.

4. MULTIVARIABLE INTEGRAL LQG CONTROLLER DESIGN

One prerequisite to achieving squeezed states of light is that the optical resonator cavity needs to be frequency-locked. In Sayed Hassen et al. [2010] and Sayed Hassen and Petersen [2010b], we assumed that the incoming beams and the intracavity fields are at resonance and the control problem then was simply one of regulating the phase of the second harmonic input field to optimise the level of squeezing achieved in the amplitude quadrature of the fundamental output field. Here, we consider the more general problem of optimising the observed level of squeezing with the OPO when the detuning variables Δ_a and Δ_b are not zero; i.e., the system is not frequency-locked. We design a multivariable controller that will regulate the detuning variables Δ_a and Δ_b along with the original requirement to regulate the phase of the incoming harmonic field. Given the strong nonlinearity associated with the frequency locking problem (see Sayed Hassen and Petersen [2010a]), here we will only consider the local behaviour of the OPO. In other words, we assume that the system is operating within the linear region of operation of the resonator cavity and that the frequency-locking requirement is to control small variations of Δ_a and Δ_b about $\Delta_a = \Delta_b = 0$.

4.1 Problem Setup

The OPO is exposed to fixed dc and low frequency disturbances in addition to high frequency noises. In this case, we will consider two separate sources of mechanical noises acting on the OPO. One of these will offset the detuning variables Δ_a and Δ_b and the other one will adversely influence the phase of the second harmonic input field $\hat{B}_{in}$. Mechanical noises at the mirrors result in variation in the optical path length which in turn affect Δ_a and Δ_b. Since in this case, one mirror is used to control both detuning variables, it can be easily shown that small variations in the optical length of the cavity result in detuned variables which share the following relationship:

$$\Delta_b = 2\Delta_a. \tag{14}$$

We will use this linear relationship between the detuning variables to simplify the design problem as regulating one of the detuning variables to zero is equivalent to regulating both to zero. The dynamical equations describing the linear behaviour of the OPO (6)-(11) can thus be rewritten using either Δ_a or Δ_b. We shall use Δ_a from this point onwards.

The measurements we use are the amplitude quadrature of the fundamental output field δX^+_{Aout} and the phase quadrature of the second harmonic output field δX^-_{Bout}. Actuation is provided by two piezo-electric actuators acting on the two mirrors in Fig. 1, thus regulating the detuning variables $\Delta_a(\Delta_b)$ and the phase quadrature of the second harmonic input field, δX^-_{Bin}. In Fig. 1, the rightmost mirror is chosen as the point of actuation for the control of the detuning variables Δ_a (Δ_b). The piezo-electric actuator attached to the mirrors (the mechanical subsystems) are modelled as second-order systems. The dynamics of the actuator used to control the phase of the second harmonic input field are described by:

$$\begin{aligned}\begin{bmatrix}\dot{\xi}_1\\ \dot{\xi}_2\end{bmatrix} &= \begin{bmatrix}0 & 1\\ -r_2 & -r_1\end{bmatrix}\begin{bmatrix}\xi_1\\ \xi_2\end{bmatrix} + \begin{bmatrix}0\\ 1\end{bmatrix} w_1 + \begin{bmatrix}0\\ 1\end{bmatrix} u_2;\\ \delta X^-_{Bin} &= \begin{bmatrix} c_2 & c_1 \end{bmatrix}\begin{bmatrix}\xi_1\\ \xi_2\end{bmatrix} + p_{B,in}.\end{aligned} \tag{15}$$

Similarly, the actuator used to control the detuning variables Δ_a and Δ_b can be described as follows:

$$\begin{aligned}\begin{bmatrix}\dot{\xi}_3\\ \dot{\xi}_4\end{bmatrix} &= \begin{bmatrix}0 & 1\\ -r_4 & -r_3\end{bmatrix}\begin{bmatrix}\xi_3\\ \xi_4\end{bmatrix} + \begin{bmatrix}0\\ 1\end{bmatrix} w_2 + \begin{bmatrix}0\\ 1\end{bmatrix} u_1;\\ \Delta_a &= \begin{bmatrix} c_4 & c_3 \end{bmatrix}\begin{bmatrix}\xi_3\\ \xi_4\end{bmatrix} + p_0.\end{aligned} \tag{16}$$

Here, ξ_1, ξ_3 represent deviations in the position of the mirrors which control the phase of the second harmonic input field and the detuning variables respectively. Also, ξ_2, ξ_4 represent the velocities of the mirrors. The quantities w_1 and w_2 represent process noises which arise due to mechanical fluctuations in the beam path and $p_{B,in}$ and p_0 represent quantum noises. The complete linearised system can then be represented in state-space form as:

$$\dot{x} = Ax + B_1 u + B_2 w; \tag{17}$$

$$y = Cx + Dw; \tag{18}$$

$$\Delta_a = Fx, \tag{19}$$

where

$$x = \begin{bmatrix} \delta X^+_a & \delta X^-_a & \delta X^+_b & \delta X^-_b & \xi_1 & \xi_2 & \xi_3 & \xi_4 \end{bmatrix}^T;$$

$$w = \Big[\delta X^+_{Ain}\ \ \delta X^-_{Ain}\ \ \delta X^+_{Bin}\ \ p_{B,in}\ \ p_0\ \ X^+_{\delta A,l}\ \ X^-_{\delta A,l}\ \ X^+_{\delta B,l}\ \ X^-_{\delta B,l}\ \ w_1\ \ w_2\Big]^T;$$

$$u = [u_1\ \ u_2]^T; \quad y = \left[\delta X^-_{Bout}\ \ \delta X^+_{Aout}\right]^T.$$

4.2 LQG Performance Criterion and Integral Action

The performance requirement to minimise the variance of the amplitude quadrature of the fundamental output field $\hat{A}_{out}$ as specified in Sayed Hassen et al. [2010], is in this case supplemented with the additional requirement to minimise the detuning variables Δ_a and Δ_b. An arbitrary quadrature, X^θ, can be described as (see Bachor and Ralph [2004]):

$$X^\theta = X^+ \cos\theta + X^- \sin\theta. \tag{20}$$

We can thus define the control variables as:

$$z_1 = \delta X^+_a \cos\bar{\theta}_{a,out} + \delta X^-_a \sin\bar{\theta}_{a,out}; \tag{21}$$

$$z_2 = \Delta_a. \tag{22}$$

Moreover, due to the presence of dc and low frequency noises, there is a need to include integral action in the LQG controller design process. In this problem, there are two sources of low frequency noises, as described in Sec. 4.1. The standard LQG cost functional is thus modified to include an additional term which involves the integral of the outputs. Let us introduce the integral operator L where,

$$L(y) = \begin{bmatrix} L(y_1) \\ L(y_2) \end{bmatrix} = \begin{bmatrix} \int_0^T y_1(\tau)\, d\tau \\ \int_0^T y_2(\tau)\, d\tau \end{bmatrix}. \tag{23}$$

We can now formulate the integral LQG performance criterion as the minimisation of the following cost function:

$$\mathcal{J} = \lim_{T\to\infty} \mathbf{E}\left[\frac{1}{T}\int_0^T x^T Q x + L(y)^T \bar{Q} L(y) + u^T R u\, dt\right]. \tag{24}$$

We choose the matrices Q, $\bar{Q}$, and R such that:

$$x^T Q x = x^T \begin{bmatrix} q_1 & 0 \\ 0 & q_2 \end{bmatrix} x = q_1|z_1|^2 + q_2|z_2|^2;$$

$$L(y)^T \bar{Q} L(y) = L(y)^T \begin{bmatrix} q_3 & 0 \\ 0 & q_4 \end{bmatrix} L(y) = q_3|L(y_1)|^2 + q_4|L(y_2)|^2;$$

$$u^T R u = u^T \begin{bmatrix} r_{w1} & 0 \\ 0 & r_{w2} \end{bmatrix} u = r_{w1}|u_1|^2 + r_{w2}|u_2|^2.$$

Here, q_1, q_2, q_3, q_4, r_{w1}, $r_{w2} > 0$ are treated as design parameters. The expectation in (24) is with respect to the Gaussian quantum and classical noise processes, and the assumed Gaussian initial conditions. The underlying assumption here is that the conditional state associated with a quantum system can be equivalently modelled using a classical system; see Edwards and Belavkin [2005].

Fig. 2 shows the set-up used for the multivariable integral LQG controller design. In order to apply the standard

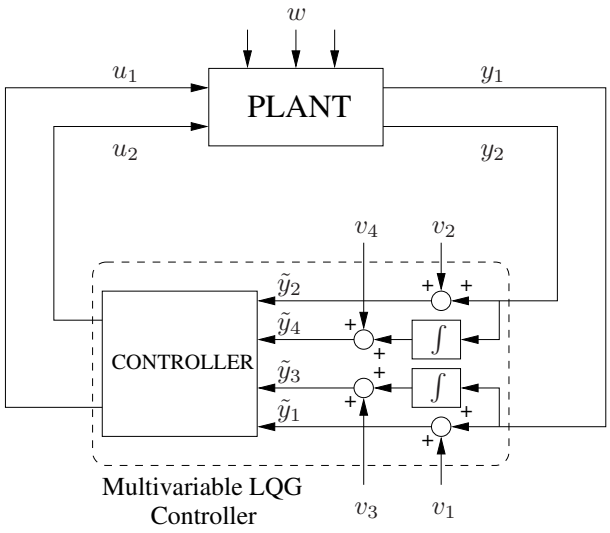

Fig. 2. Multivariable controller design configuration.

LQG technique to this system, we include the integrators as part of an augmented system which we define next. If we let

$$\tilde{x} = \begin{bmatrix} x \\ L(y) \end{bmatrix};\ \ \tilde{y} = \begin{bmatrix} \tilde{y}_1 \\ \tilde{y}_2 \\ \tilde{y}_3 \\ \tilde{y}_4 \end{bmatrix};\ \text{and}\ \ \tilde{w} = \begin{bmatrix} w \\ v_1 \\ v_2 \\ v_3 \\ v_4 \end{bmatrix};$$

we can rewrite the dynamics of the complete system as

$$\dot{\tilde{x}} = \tilde{A}\tilde{x} + \tilde{B}_1 u + \tilde{B}_2 \tilde{w}; \tag{25}$$

$$\tilde{y} = \tilde{C}\tilde{x} + \tilde{D}\tilde{w}. \tag{26}$$

Here,

$$\tilde{A} = \begin{bmatrix} A & 0 \\ C & 0 \end{bmatrix};\ \ \tilde{B}_1 = \begin{bmatrix} B_1 \\ 0 \end{bmatrix};\ \ \tilde{B}_2 = \begin{bmatrix} B_2 & 0 \\ D & 0 \end{bmatrix}; \tag{27}$$

$$\tilde{C} = \begin{bmatrix} C & 0 \\ 0 & I \end{bmatrix};\ \ \tilde{D} = \begin{bmatrix} D \\ 0 \end{bmatrix} \begin{bmatrix} 0 & I_{4\times 4} \end{bmatrix}. \tag{28}$$

After the controller design, the integrators are pulled back from the augmented system and are included as part of the controller, as shown in Fig. 2. The performance criterion can now be reformulated as:

$$\mathcal{J} = \lim_{T\to\infty} \mathbf{E}\left[\frac{1}{T}\int_0^T \tilde{x}^T \tilde{Q} \tilde{x} + u^T R u\, dt\right], \tag{29}$$

where

$$\tilde{Q} = \begin{bmatrix} Q & 0 \\ 0 & \bar{Q} \end{bmatrix}. \tag{30}$$

The multivariable controller is constructed by estimating the states of the augmented system described by (25) using a Kalman filter and combining it with an optimal state feedback control law as follows:

$$u = -K\hat{\tilde{x}}.$$

The optimal feedback gain matrix is given by

$$K = R^{-1}\tilde{B}_1^T X,$$

where X satisfies the matrix Riccati equation:

$$\bar{Q} - R^{-1}X\tilde{B}_1\tilde{B}_1^T X + X\tilde{A} + \tilde{A}^T X = 0. \quad (31)$$

The optimal observer dynamics (Kalman filter) are described by

$$d\hat{\tilde{x}} = \tilde{A}\hat{\tilde{x}}\,dt + \tilde{B}_1 u\,dt + L[d\tilde{y} - \tilde{C}\hat{\tilde{x}}\,dt]; \quad (32)$$

and the solution of the optimal observer is obtained by choosing the gain matrix

$$L = (P_e\tilde{C}^T + \tilde{B}_2\tilde{D}^T)(\tilde{D}\tilde{D}^T)^{-1}, \quad (33)$$

where P_e is the solution to the matrix Riccati equation

$$\begin{aligned}(\tilde{A} - \tilde{B}_2\tilde{D}^T(\tilde{D}\tilde{D}^T)^{-1}\tilde{C})P_e \\ + P_e(\tilde{A} - \tilde{B}_2\tilde{D}^T(\tilde{D}\tilde{D}^T)^{-1}\tilde{C})^T \\ - P_e\tilde{C}^T(\tilde{D}\tilde{D}^T)^{-1}\tilde{C}P_e + \tilde{B}_2\tilde{B}_2^T \\ - \tilde{B}_2\tilde{D}^T(\tilde{D}\tilde{D}^T)^{-1}\tilde{D}\tilde{B}_2^T = 0. \quad (34)\end{aligned}$$

4.3 Model and Design Parameters

The parameter values we used were chosen to reflect those of an optical squeezer in our optics laboratory (see Heurs et al. [2009]) and are shown in Table 1.

Model parameter	Value	Units
κ_a	1×10^5	rad/s
κ_b	1×10^9	rad/s
$\kappa_{a,l}$	5×10^3	rad/s
$\kappa_{b,l}$	5×10^7	rad/s
$\kappa_{a,in}$	9.5×10^4	rad/s
$\kappa_{b,in}$	9.5×10^8	rad/s
$\chi^{(2)}$	3×10^{-2}	–
$\bar{A}_{in}$	2×10^6	$\sqrt{\text{rad/s}}$
$\bar{B}_{in}$	2×10^{10}	$\sqrt{\text{rad/s}}$

Table 1. Model parameter values of the OPO.

The parameter values of the piezo-electric actuators and the steady-state phase angles of the input fields used for the controller design are shown in Table 2.

Model parameters			
r_1	8×10^3	r_2	1×10^9
c_1	-5×10^3	c_2	1.5×10^{10}
r_3	5×10^4	r_4	3×10^9
c_3	-4×10^3	c_4	3×10^{10}
$\bar{\theta}_{a,in}$	$\pi/3$	$\bar{\theta}_{b,in}$	$5\pi/3$

Table 2. Model parameters of the piezo-electric actuators and input laser beam phase.

Table 3 shows the design parameters used for the generation of the LQG controller. The quantity ϵ_{qn}^2 represents the quantum noise variance, ϵ_{w1}^2 and ϵ_{w2}^2 represent the variance of the process noises feeding into the respective piezo-electric actuators, and $\epsilon_{p_{B,in}}^2$ and $\epsilon_{p_0}^2$ model the respective sensor noise variances acting on the piezo-actuators. Also, $\epsilon_{v1}^2, \epsilon_{v2}^2, \epsilon_{v3}^2$ and ϵ_{v4}^2 are used to model the variance of the sensor noise on the 4 measurements $\tilde{y}_1, \tilde{y}_2, \tilde{y}_3$ and $\tilde{y}_4$. In particular, note that the sensor noises present in $\tilde{y}_3$ and

Design Parameters			
q_1	1×10^{10}	q_2	1×10^8
q_3	5×10^{15}	q_4	5×10^{15}
r_{w1}	5×10^{10}	r_{w2}	3×10^8
ϵ_{qn}	1	ϵ_{w1}	1
ϵ_{w2}	1	$\epsilon_{p_{B,in}}$	$\sqrt{10}$
ϵ_{p_0}	1	ϵ_{v1}	1
ϵ_{v2}	1×10^{-2}	ϵ_{v3}	1×10^{-6}
ϵ_{v4}	1×10^{-6}		

Table 3. Multivariable LQG controller design parameters.

$\tilde{y}_4$ are fictitious and are included for design purposes only. These parameters were adjusted until a suitable controller was obtained.

We then confirm the closed-loop stability of the multivariable system by using MacFarlane's characteristic loci test; see Desoer and Wang [1980]; MacFarlane and Belletrutti [1973]. The characteristic loci test is a generalisation of the Nyquist plot, which arises as a special scalar case of this approach. As is done in the scalar case, we calculate the multivariable loop gain transfer function matrix

$$L(j\omega) = -P(j\omega)K(j\omega) = \begin{bmatrix} L_{11}(j\omega) & L_{12}(j\omega) \\ L_{21}(j\omega) & L_{22}(j\omega) \end{bmatrix}, \quad (35)$$

over a suitable range of frequency. Here P and K represent the dynamics of the plant and the controller respectively. The characteristic loci test then involves computing the eigenvalues of this matrix at each frequency ω and then plotting the loci of these eigenvalues in the complex plain. Since both the plant and the controller are stable, the characteristic loci in our case guarantees stability if there are no net encirclements of the $-1+j0$ point. This result is confirmed in Fig. 3 where we show the characteristic locus of the two eigenvalues of $L(j\omega)$.

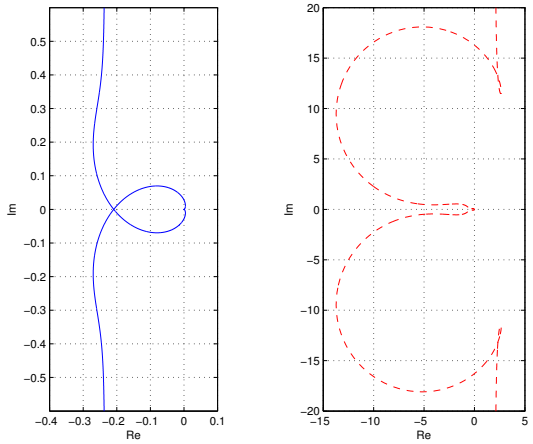

Fig. 3. Characteristic loci plot of $L(j\omega)$.

5. SIMULATION RESULTS

Using the model parameters in Tables 1 and 2, we then simulate the system using SIMULINK®. The laser noises used in the simulation are modelled as (approximately) integrated white noise superimposed over a fixed dc offset. They are described by the following transfer functions:

$$P_{ln1}(s) = \frac{k_1}{\tau_1 s + 1} \quad \text{and} \quad P_{ln2}(s) = \frac{k_2}{\tau_2 s + 1}, \qquad (36)$$

respectively, where $k_1 = 6.67 \times 10^7, \tau_1 = 3.33 \times 10^4, k_2 = 7.5 \times 10^7$, and $\tau_2 = 5 \times 10^4$. The initial position of the mirrors introduce constant offsets in frequency and in phase for the cavity mirror and the phase controlling mirror respectively. We consider the case where the system is excited with both classical and quantum noises and simulate the closed-loop system to show the performance of the designed controller.

Fig. 4 shows the movement of the mirrors compensating for the noises acting on the system. We note that mirror 2 controlling the phase quadrature of the input field is more sensitive to noise. Once the detuning variables stabilise and the system is in or close to frequency-lock, the phase quadrature of the input field is better regulated by mirror 2. This result is as expected since squeezing can be achieved only in a frequency-locked cavity.

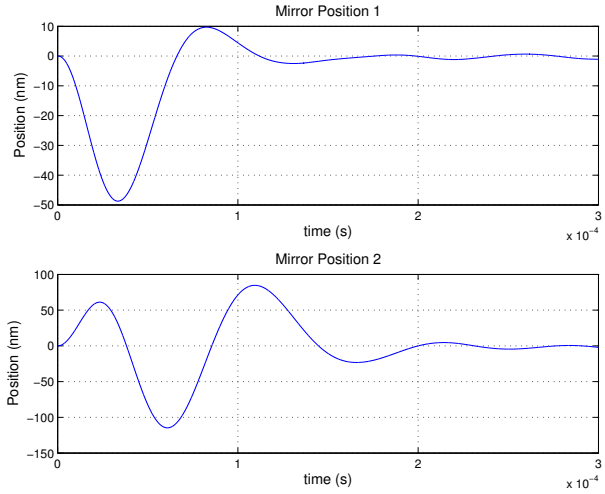

Fig. 4. Mirror positions 1 and 2.

Finally, we also simulate the open-loop and closed-loop system to compare the effect of having no controller on the filtered controlled variable z_1. Fig. 5 compares the time history for the two cases.

6. CONCLUSION AND FUTURE WORK

In this paper, we designed a multivariable controller to obtain optimal squeezing by regulating both the detuning variables and the phase of an incoming optical field. We showed that depending on the phase of the input optical fields, we can determine the type and the extent of squeezing observed. We considered a realistic situation with the optical cavity operating away from resonance; i.e., the detuning variables being non-zero and two separate sources of mechanical noises with dc offsets acting at different locations on the system. A multivariable controller is designed and successfully simulated with piezo-electric actuators controlling the position of the two mirrors. Future work would involve implementing the proposed control approach on an experimental test bed. Another avenue for future research could also investigate the possibility of achieving a global lock for the optical resonator cavity, as was done in Sayed Hassen and Petersen [2010a].

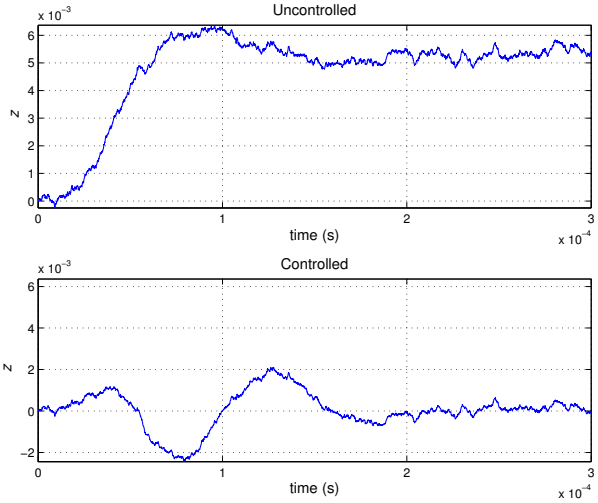

Fig. 5. The uncontrolled and controlled variable z_1

REFERENCES

H. A. Bachor and T. C. Ralph. *A Guide to Experiments in Quantum Optics*. John Wiley, 2004.

R. W. Boyd. *Nonlinear Optics*. Academic Press, Boston, 2008.

C. M. Caves. Quantum-mechanical noise in an interferometer. *Phys. Rev. D*, 23(8):1693–1708, Apr 1981.

M. J. Collett and C. W. Gardiner. Squeezing of intracavity and traveling-wave light fields produced in parametric amplification. *Phys. Rev. A*, 30(3):1386–1391, Sep 1984.

C. A. Desoer and Y-T. Wang. On the Generalized Nyquist Stability Criterion. *IEEE Trans. Autom. Control*, 25(2): 187–196, April 1980.

S. C. Edwards and V. P. Belavkin. Optimal quantum feedback control via quantum dynamic programming. arXiv:quant-ph/0506018, 2005.

C. W. Gardiner and P. Zoller. *Quantum Noise*. Springer, Berlin, 2000.

M. Heurs, I. R. Petersen, M. R. James, and E. H. Huntington. Homodyne locking of a squeezer. *Optics Letters*, 34(16):2465–2467, Aug. 2009.

A. G. J. MacFarlane and J. J. Belletrutti. The Characteristic Locus Design Method. *Automatica*, 9(5):575–588, Sept. 1973.

S. Z. Sayed Hassen and I. R. Petersen. A time-varying Kalman filter approach to integral LQG frequency locking of an optical cavity. In *Proc. American Control Conf.*, pages 2736–2741, Baltimore, MD, USA, July 2010a.

S. Z. Sayed Hassen and I. R. Petersen. Optimal amplitude quadrature control of an optical squeezer using an integral LQG approach. In *IEEE Multi-Conference on Systems and Control*, pages 286–291, Yokohama, Japan, Sept. 2010b.

S. Z. Sayed Hassen, M. Heurs, E. H. Huntington, I. R. Petersen, and M. R. James. Frequency Locking of an Optical Cavity using Linear-Quadratic Gaussian Integral Control. *J. Phys. B: At. Mol. Opt. Phys.*, 42 (17):175501, Sept. 2009.

S. Z. Sayed Hassen, I. R. Petersen, E. H. Huntington, M. Heurs, and M. R. James. LQG control of an optical squeezer. In *Proc. American Control Conf.*, pages 2730–2735, Baltimore, MD, USA, July 2010.